

## NUMERICAL STUDY OF THE STOPPING OF AURA DURING MIGRAINE

C. POCCHI<sup>1</sup>, A. MOUSSA<sup>2</sup>, F. HUBERT<sup>3</sup> AND G. CHAPUISAT<sup>4</sup>

**Abstract.** This work is devoted to the study of migraine with aura in the human brain. Following [6], we class migraine as a propagation of a wave of depolarization through the cells. The mathematical model used, based on a reaction-diffusion equation, is briefly presented. The equation is considered in a duct containing a bend, in order to model one of the numerous circumvolutions of the brain. For a wide set of parameters, one can establish the existence of a critical radius below which the wave stops. The approximation scheme used for the simulations is first described and then a numerical study is realized, precisising the dependence of the critical radius with respect to the different parameters of the model.

**Résumé.** Ce travail est consacré à l'étude de l'évolution d'une migraine avec aura dans le cerveau humain. Suivant [6], nous assimilons la migraine à une onde de dépolarisation attaquant les cellules du cerveau. Le modèle mathématique retenu, basé sur une équation de réaction-diffusion, est brièvement rappelé. Le domaine d'espace utilisé est constitué d'un conduit présentant un coude, afin de représenter l'une des nombreuses circonvolutions cérébrales. Pour une importante classe de paramètres, il est possible de mettre en évidence l'existence d'un rayon critique au delà duquel le front d'onde n'arrive pas à dépasser le coude. Après une description du schéma d'approximation utilisé, une étude numérique a été réalisée, visant à préciser la dépendance du rayon critique en fonction des différents paramètres du modèle.

### INTRODUCTION

Migraine is a severe case of unilateral headache, often increased by classical symptoms like photophobia or nausea. In the specific case of migraine with aura, some symptoms appear before the crisis announcing its beginning. More than 30% of people who suffer migraine headache perceive an aura. They experience alterations in feelings and bodily perceptions: weakness, numbness of one side of the face, visual, auditory or olfactory hallucinations, temporary aphasia, vertigo, tingling in arms and legs (see figure 1 for a visual example). These symptoms gradually appear less before the headache and may last from five to twenty minutes, or may continue even after the headache subsides.

The understanding of the migraine phenomenon could help to prevent and heal it better, but it's a rather complex problem for which the simple question: "*physiologically, what is happening during a migraine with aura ?*" is still open. However, a few theories exist to answer to it. One of them is based on the concept of **Cortical Spreading Depression** (CSD), first introduced by Leão in [5]. Leão observed experimentally in 1944, on

---

<sup>1</sup> Dipartimento di Scienze di Base e Applicate per l'Ingegneria, Sezione di Matematica, Sapienza Università di Roma, Via A. Scarpa 16, 00161, Rome, Italy. E-mail: pocci@dmmm.uniroma1.it

<sup>2</sup> CMLA, ENS Cachan, CNRS, Pres UniverSud, 94235 Cachan, France

<sup>3</sup> LATP, UMR 6632, Université de Provence, CMI, 39 rue Joliot-Curie 13453 Marseille Cedex 13, France

<sup>4</sup> LATP, UMR 6632, Université Paul Cézanne Aix-Marseille 3, av Escadrille Normandie-Niemenn 13397 Marseille Cedex 20, France



FIGURE 1. Scintillating scotoma is the most common visual aura preceding migraine.

different animal species, a wave of cellular depolarization through the brain. Since then, the literature produced a high number of articles raising the CSD as a possible cause of the human migraine with aura. Of course, the extrapolation from CSD in animals to migraine for human is not straightforward, but similarities between the two phenomena are numerous [9, 10, 12, 13]. In fact, even the *existence* of spreading depressions for the human brain is discussed ([1, 8, 14] for example). Its experimental observation in the human cortex could obviously give a straight answer, but has not yet been accomplished (except for severe case of ischemic stroke [3]), as *in vivo* measurements are difficult to perform on a human patient. However, it is experimentally established that human migraine corresponds to a progressive neuronal disturbance (associated to the evolution of the different auras), evolving with the same rate as the CSD of Leão (i.e. 3mm/min), hence studying the CSD could be a lead to a further understanding of migraine with aura.

An intriguing fact is that the evolution of the aura (*i.e.* the wave of neural disturbance) is highly dependent on the considered patient. Sometimes the wave stops in a given point of the brain and may correspond to the different auras observed. The question is then: why does this wave stop? Where? If we admit that migraine corresponds with a CSD, can we recover this behaviour? As we will see further, the geometry of the human brain may answer partially to all these questions, but let us before make a few recall on the morphology of the human brain.

The cerebral cortex is the outermost layer of the brain; it's often called the *grey matter*, because in preserved brain it acquires this specific color. This grey matter contains neurons (excitable cells of the nervous system, “containing” the information) and their fibers. Below the cortex, the *white matter* is principally formed by axons (“transporting” the information). Whereas for animal species like rats for instance, the grey matter is a rather regular convex region, for the human it is filled in by circumvolutions (see figure 2).



FIGURE 2. Adult rat (left) and human (right) brains. The human brain geometry is remarkably more complex.

Though the migraine may stop at different positions in the cortex, depending on the patient, it is experimentally established that the wave always stops before a peculiar circumvolution: the *Rolando fissure* or *central sulcus* (see figure 3).

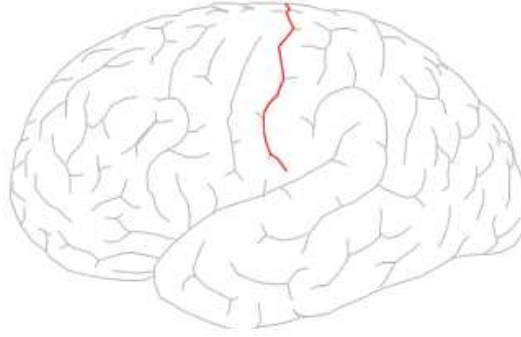


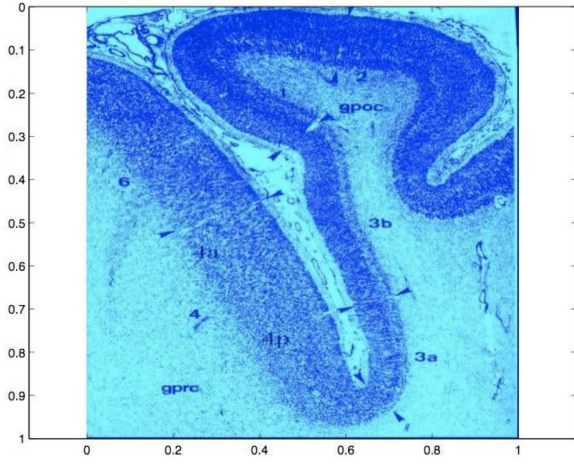
FIGURE 3. The Rolando sulcus, a double S-shaped fissure that extends obliquely upward and backward on the lateral surface of each cerebral hemisphere of the brain, located at the boundary between the frontal and parietal lobes.

If one admits that the migraine does correspond to the propagation of a wave (which would be a wave of depolarization in the case of CSD), the issue reduces to understand the role of the geometry and specially the curvature in the evolution of a travelling front. Following this remark Dronne, Grenier *et. al.* elaborated in [6] a mathematical model and a numerical study of the blocking of migraine by the central sulcus. The considered model uses the so called reaction-diffusion equation, which is known to describe quite properly progressive waves. Rather than a binary state for the neurons (*i.e.* disturbed because of the aura or not), this model assumes that they continually evolve from the normal state to the ill one (*i.e.* depolarized in the case of CSD). A **state function** is therefore defined, assumed to be equal to 0 in a normal tissue and to 1 if this tissue is completely depolarized (*i.e.* the aura is at its peak). This state function is the unknown of the model, solution to the reaction-diffusion equation for which the parameters still have to be fixed.

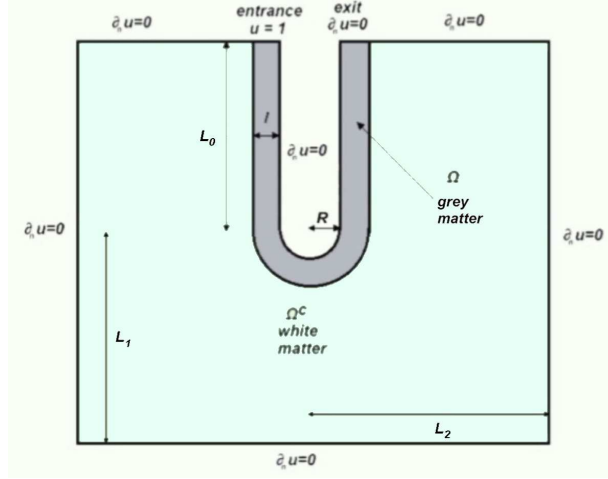
Using this model, the authors of [6] proved numerically (in 2D) the existence of parameters for which the travelling front stops because of the central sulcus. In [11] a similar model is revisited, but in a domain with only grey matter; the wave is studied in a cylindrical domain, which section may vary. Two cases are studied: sudden change of radius, and linear change of radius. In both cases, the authors made numerical experiments with different parameters and studied the critical radii and angles allowing the wave to propagate after the change of section.

Theoretical study of reaction-diffusion is well known for classical nonlinearities in “simple” domains. As soon as the nonlinearity or the domain is a little bit complex, the proof of existence and even the definition of travelling fronts is a hard challenge. This justifies the “numerical strategy” that was used in [6, 11] which may lead, after, to more theoretical results. We have followed this methodology in our study, and obtained numerical results that emphasize the role of the geometry in the wave. The propagation of a wave in a duct containing a bend is studied. For a large number of parameters set we exhibit a critical radius that stops the front wave. We have then studied the influence of this critical radius with respect to some parameters of our model.

This paper is organized as follows. In the first Section, we recall the mathematical model given in [6]. We explain in detail the numerical scheme used to approach the equation. In the second Section, we study numerically the influence of the parameters of the model on the propagation of travelling front. Finally we discuss these results and the numerical and theoretical issues that may be purchased after our study in the third Section.



(a) Zoom on a slice of brain.



(b) Numerical domain

FIGURE 4. The complex geometry of a sulcus of a brain around the interface between white and grey matter.

## 1. MATHEMATICAL MODEL

### 1.1. Description of the analytical model

Following the work of [6], we introduce a state function  $u(t, x)$  that reflects the presence of the aura. We have  $0 \leq u \leq 1$  where  $u = 0$  corresponds to a normal state and  $u = 1$  expresses a peak of the aura. The depolarization responsible for the aura is modelled by a bistable reaction-diffusion in the grey matter when the ionic species responsible for the depolarization diffuse and are absorbed in the white matter. Hence the variation of  $u$  can be described by the following reaction-diffusion equation:

$$u_t - \nu \Delta u = f(u) := bu(u - \theta)(1 - u)\chi_\Omega - \alpha u\chi_{\Omega^c} \quad \text{on } \Omega \cup \Omega^c, \quad (1)$$

where  $\chi_D$  is the characteristic function of a domain  $D$ ,  $\Omega$  is the grey matter of the brain and  $\Omega^c$  is the white matter,  $\nu$  is the diffusive coefficient supposed constant,  $b$  is the amplification coefficient of the grey matter,  $\theta$  is the reaction threshold of the grey matter and  $\alpha$  is the absorption coefficient in the white matter.

### 1.2. Numerical domain

Figure 4(a) reveals a complex geometry of the grey matter. As we want to understand the influence of this complex geometry on the spreading of the depolarization wave responsible for the aura, we propose to work in the geometry represented by figure 4(b). This geometry is characterized by the parameters  $R$ ,  $l$ ,  $L_0$ ,  $L_1$  and  $L_2$ . The domain is composed by two subdomains,  $\Omega$  and  $\Omega^c$ .  $\Omega$  is a U-shaped domain corresponding to the grey matter whereas  $\Omega^c$  shown in the figure 4(b) represents the white matter. In this paper we will pay a particular attention to the influence of the radius  $R$  on the propagation of the aura.

We impose homogeneous Neumann boundary conditions on  $\partial(\Omega \cup \Omega^c) \setminus \Gamma$ , where  $\Gamma$  is a part of  $\partial\Omega$  that we call the entrance. On  $\Gamma$  we impose  $u = 1$ .

$$\frac{\partial u}{\partial n} = 0 \quad \text{on } \partial(\Omega \cup \Omega^c) \setminus \Gamma, \quad u = 1 \quad \text{on } \Gamma. \quad (2)$$

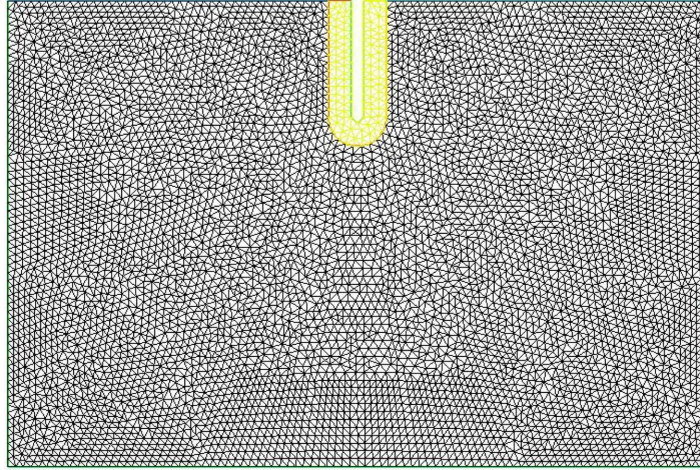


FIGURE 5. Uniform mesh used for our study.

We start from  $u = 0$  on  $\Omega \cup \Omega^c$ . The boundary condition on  $\Gamma$  ensures the propagation of a generalized travelling front for a short time. The long time propagation of such a wave depends on the values of the parameters of the model  $b, \alpha, \theta, \nu$  and the radius  $R$  of the circumvolution.

The theoretical understanding of the wave propagation on such a domain is a difficult problem and its numerical understanding will be of great importance in the further development of the theory.

### 1.3. Discretization of the model

The equation (1) is discretized in time by a semi-implicit Euler scheme.

$$\frac{u^{m+1} - u^m}{dt} - \nu \Delta u^{m+1} = f(u^m), \quad (3)$$

where  $f$  is defined in (1). Simulations are made on FreeFem++, Third edition, Version 3.3-3 ([7]). P1 finite elements method is used for the space discretization. Note that the characteristic functions  $\chi_\Omega$  and  $\chi_{\Omega^c}$  are discretized by P0 elements. We observed that under the condition

$$dt < \min \left\{ \frac{1}{b\theta}, \frac{1}{\alpha} \right\}, \quad (4)$$

the scheme remains stable. This condition is derived from the stability of the explicit Euler scheme of the ordinary differential equations  $u_t = bu(u - \theta)(1 - u)$  and  $u_t = -\alpha u$ . We devote great attention to the quality of the mesh, due to the complexity of the geometry (see figure 5). Since the boundary conditions are unnatural, we have to choose  $L_0, L_1$  and  $L_2$  sufficiently large to avoid interference of the boundary on the propagation of the wave. In the following, we have taken  $L_0 = 1$  and  $L_1 = L_2 = 5$ . Moreover, by a change of scale, the diffusion coefficient  $\nu$  can be assumed equal to 0.1 and in this work we will take  $l = 0.2$ . We want now to study the influence of  $b, \theta, \alpha$  and  $R$  on the propagation of the travelling front.

## 2. INFLUENCE OF THE DIFFERENT PARAMETERS

Let us define for  $b > 0, \theta \in ]0, 1/2[$  and  $\alpha > 0$ , the *critical radius*  $R_c(b, \theta, \alpha) \in [0, +\infty[$  such that for  $R < R_c$  the wave stops, otherwise it does not. The existence of such a unique threshold between propagation or not

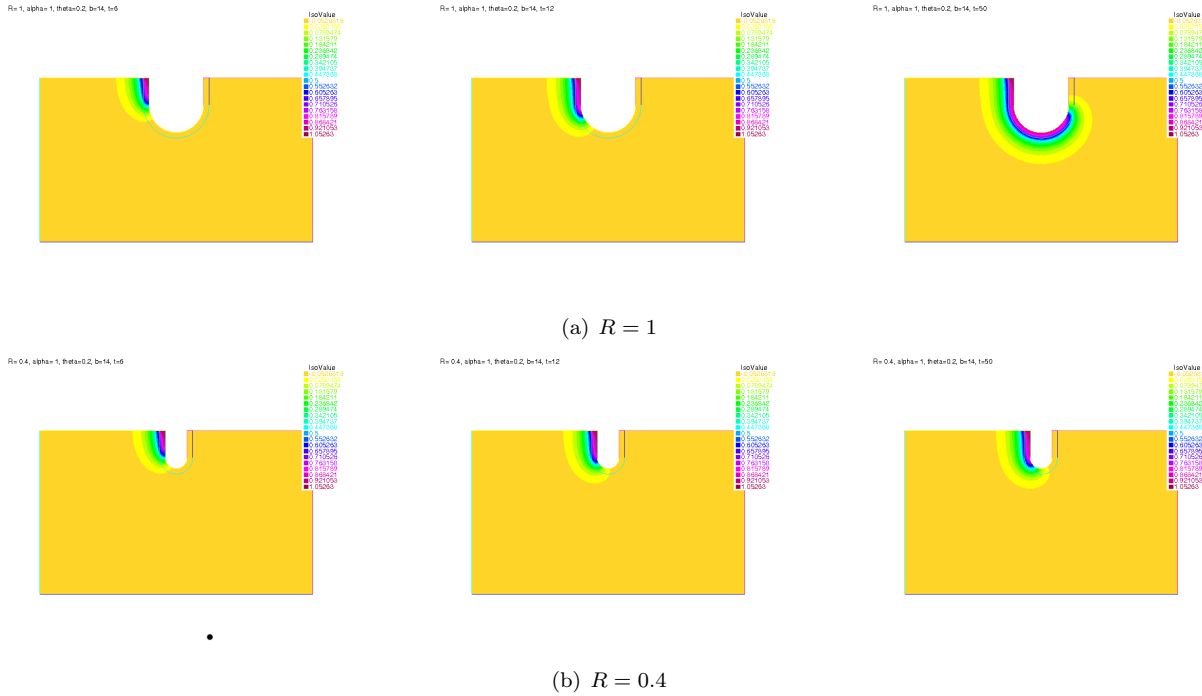


FIGURE 6. The solution  $u$  at different times ( $t = 6, t = 12, t = 50$  from left to right) and for different radii  $R$ .

is still not proved, however the numerical experiments that we have made lead us to be inclined to favour the existence of such a critical radius.

It has already been proved that no travelling wave can propagate on a straight cylinder of grey matter with white matter outside if  $l$  is small enough and that travelling fronts exist if  $l$  is large enough [4]. This limit value of  $l$  depends on  $b, \theta$  and  $\alpha$ . Hence there exist values of  $b, \theta$  and  $\alpha$  such that  $R_c(b, \theta, \alpha) = +\infty$ . We assume that there also exist sets of parameters values such that  $R_c = 0$ , *i.e.* for any value of  $R$  the travelling front will cross the U-turn. This point however is still an open question. In the following, we want to determine for a large set of values of parameters  $b, \theta$  and  $\alpha$  if the critical radius  $R_c$  belongs to  $]0, +\infty[$  and how it depends on these parameters.

First we have to specify a numerical criterium that ensures the stopping of the wave. As the numerical scheme we use is of order 1 with respect to the time step  $dt$  and the space discretization step  $h$ , we will say that the wave stops as soon as

$$\frac{\|u^m\|_\infty}{\|u^{m+1}\|_\infty} < \min(dt^2, h^2). \tag{5}$$

We call *stopping set* a set of values of parameters for which the wave stops as for example (figure 6(b)):

$$b = 14, \quad \theta = 0.2, \quad \alpha = 1, \quad R = 0.4. \tag{6}$$

Similarly we call *passing set* a set of values of parameters for which the wave passes as for example (figure 6(a)):

$$b = 14, \quad \theta = 0.2, \quad \alpha = 1, \quad R = 1.$$

The numerical solution at different times for those two sets of parameters is presented on figure 6. In both cases, the wave is slowed down when it reaches the U-turn. Now for  $R = 1$  (figure 6(a)), the speed of the wave

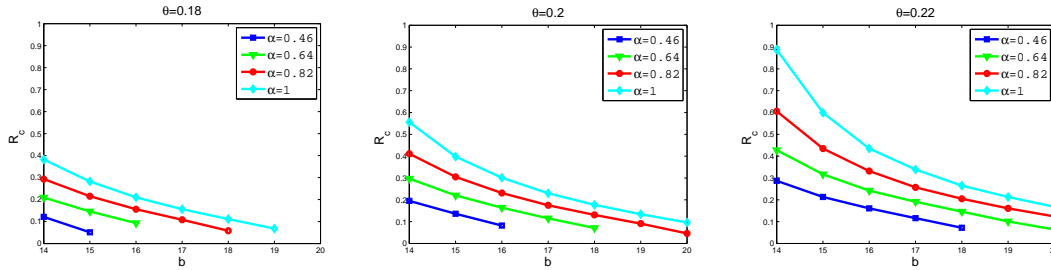


FIGURE 7. Behaviour of  $R_c$  depending on  $b$  for various values of  $\alpha$  and  $\theta$ . Critical radii  $R_c$  less than 0.1 were not computed in these simulations.

is positively bounded and the travelling front gets over the curved part of the cylinder. On the opposite, for  $R = 0.4$  (figure 6(b)), the speed of the wave tends quickly to zero and the wave stops at the entrance of the U-turn.

In the following, we will take  $b$  between  $b_{\min} = 14$  and  $b_{\max} = 20$ ,  $\alpha$  between  $\alpha_{\min} = 0.28$  and  $\alpha_{\max} = 1$  and  $\theta$  between  $\theta_{\min} = 0.15$  and  $\theta_{\max} = 0.22$ . These ranges of values of the parameters ensure the propagation of travelling front over the straight part of the cylinder ( $R_c < \infty$ ). The question is to know if the curved part of the domain will be able to stop the spreading of the wave. For such range of  $b$ , we can fix  $dt = 0.04$  to fulfill the stability condition (4).

For a fixed set of parameters  $b$ ,  $\alpha$ ,  $\theta$ , we will find values  $R_{\min}$  and  $R_{\max}$  such that the set  $\{b, \alpha, \theta, R_{\min}\}$  is a stopping set and  $\{b, \alpha, \theta, R_{\max}\}$  is a passing set. This will ensure  $R_c \in [R_{\min}, R_{\max}]$  and we will use a dichotomy algorithm to determine  $R_c(b, \alpha, \theta)$ . The precision of the dichotomy algorithm is of  $5 \cdot 10^{-4}$ . For these sets of parameters, we took  $R_{\min} = 0.02$  and  $R_{\max} = 1$ . Results are presented on figure 7.

**Proposition 2.1.**  $R_c$  is monotonically increasing with respect to the parameter  $\alpha$ .

*Proof.* The increasing behaviour of  $R_c$  depending on  $\alpha$  can be proved using the maximum principle. Let us fix  $\alpha_1 > \alpha_2 > 0$ . We denote by  $u_1$  (resp.  $u_2$ ) the solution of equation (1) with  $\alpha = \alpha_1$  (resp.  $\alpha = \alpha_2$ ). Then  $u_2$  is a supersolution of equation (1) with  $\alpha = \alpha_1$ . Since 0 is a subsolution and  $0 \leq u_2$ , by monotonicity methods we have  $u_2 \geq u_1$  and using the strong maximum principle, we can even prove  $u_2 > u_1$ . Hence if  $\{b, \alpha_2, \theta, R\}$  is a stopping set, necessarily  $\{b, \alpha_1, \theta, R\}$  is also a stopping set and we conclude that  $R_c(\alpha_2) \leq R_c(\alpha_1)$ .  $\square$

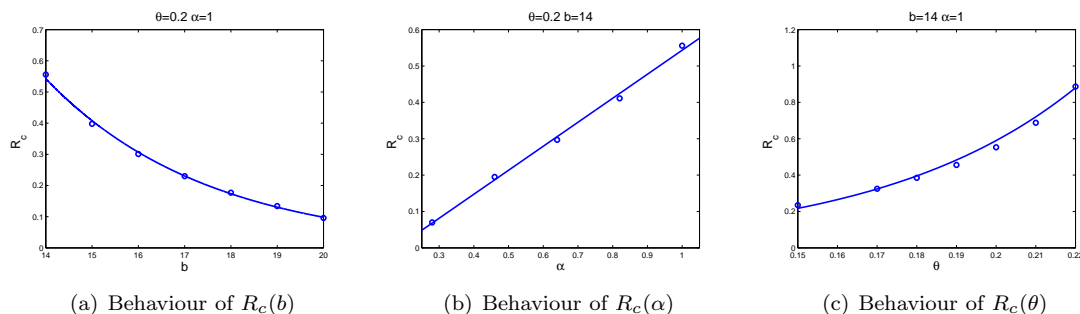
Moreover, we observe an increasing behaviour of  $R_c$  with respect to  $\theta$  and, on the opposite, a decreasing behaviour with respect to  $b$ . Although these facts are rather intuitive, the previous proof does not work since the sign of the nonlinearity is unknown.

We can also notice on figure 7 that  $R_c$  is much more sensible to changes of  $\theta$  than to changes of  $\alpha$  or  $b$ .

We have made attempts to identify more precisely the type of growth or decay of  $R_c$  with respect to each parameter. For  $\theta = 0.2$  and  $\alpha = 1$ ,  $R_c$  seems to decrease exponentially with  $b$  (figure 8(a)). For  $b = 14$  and  $\theta = 0.2$ , the behaviour of  $R_c$  depending on  $\alpha$  is rather linear (figure 8(b)). Finally, for  $b = 14$  and  $\alpha = 1$ ,  $R_c$  seems to increase rather exponentially with  $\theta$  (figure 8(c)) but the fitting of the exponential is less accurate. For other sets of parameters, the fitting with exponential or linear functions is more or less appropriate depending on the set of parameters. Specially it can be observed that when the critical radius becomes too small ( $< 0.1$ ), it seems to leave the exponential or linear behaviour.

### 3. DISCUSSION

Previous results show a strong influence of the circumvolutions of the brain on the propagation of aura during migraine and that the aura stops at the bottom of a circumvolution. The aura was modeled by a reaction-diffusion equation of bistable type coupled with a diffusion-absorption equation. The parameters of the equation

FIGURE 8. Behaviour of  $R_c$  depending on each parameter.

influence the critical radius of propagation. The results obtained are rather intuitive. Hence if we want the aura to stop earlier in less stiff circumvolution (with a larger radius), then we have to decrease the strength of the reaction term, to increase the threshold over which we have creation of depolarization or to increase the absorption effect of the white matter. These effects could be obtained by blocking the right ionic channels with the adapted therapeutic agents.

Note that many points of this study could be refined. First, the stopping criterium of the dichotomy algorithm could be decreased to improve the precision of the critical radius. Now computations are long since waves are slowed down by the U-turn and specially for values of  $R$  near the critical radius. For example in figure 6(a), computations until time 55 were needed to be sure that the wave has passed the U-turn. As well, when the radius  $R$  becomes too small, a good mesh is difficult to generate. Hence in this paper, we were not able to compute critical radii less than 0.1. We are currently working on generating refined meshes for very small radii.

We need refined computations for small radii to check what happens for critical radius  $R_c$  near to 0. The poor fitting of these values of  $R_c$  to exponential (resp. linear) functions may be related to a change of behaviour of  $R_c$  when it tends to 0. Indeed if we assume that the critical radius is simply exponentially decreasing with respect to  $b$ , but that for a large value of  $b$   $R_c = 0$  and for a small value of  $b$   $R_c = +\infty$ , there must be discontinuities for  $R_c(b)$ . This is rather unlikely but cannot be neglected. It is more likely that the behaviour is not exactly an exponential or linear function even if it is that behaviour that dominates in the range of values of parameters chosen in this paper.

Finally, a more realistic description of the human brain could be taken into account. For instance, it is well known that the permeability is discontinuous across the interface white/grey matter and that the fibers of the brain generate anisotropy in the permeability. The use of DDFV-scheme [2] would be of great interest to study the influence of heterogeneity and anisotropy in the brain.

## REFERENCES

- [1] T. Manor S. Meilin N. Zarchin A. Mayevsky, A. Doron and G. E. Ouaknine. Cortical spreading depression recorded from the human brain using a multiparametric monitoring system. *Brain Res.*, 740:268–274, 1996.
- [2] F. Boyer and F. Hubert. Finite volume method for 2d linear and nonlinear elliptic problems with discontinuities. *SIAM Journal of Numerical Analysis*, 46(6):3032–3070, 2008.
- [3] M. Fabricius B. Bosche T. Reithmeier R. I. Ernestus G. Brinker J. P. Dreier J. Woitzik C. Dohmen, O. W. Sakowitz and A. J. Strong. Spreading depolarizations occur in human ischemic stroke with high incidence. *Ann Neurol*, 63(6):720–728, 2008.
- [4] G. Chapuisat. Existence and nonexistence of curved front solution of a biological equation. *J. Differential Equations*, 236(1):237–279, 2007.
- [5] A. de A. P. Leão. Spreading depression of activity in the cerebral cortex. *Journal of Neurophysiology*, 7(6):359–390, 1944.
- [6] S. Descombes H. Gilquin A. Jaillard M. Hommel E. Grenier, M. A. Dronne and J. P. Boissel. A numerical study of the blocking of migraine by Rolando sulcus. *Progress in Biophysics and Molecular Biology*, 97(1):54–59, 2008.
- [7] K. Ohtsuka F. Hecht, A. Le Hyaric and O. Pironneau. Freefem++, finite elements software. <http://www.freefem.org/ff++/>.
- [8] A. Gorji. Spreading depression in human neocortical slices. *Brain Research*, 906:74–83, 2001.



- [9] M. Lauritzen. Cerebral blood flow in migraine and cortical spreading depression. *Acta neurologica Scandinavica. Supplementum*, 113:1, 1987.
- [10] M. Lauritzen. Pathophysiology of the migraine aura: the spreading depression theory. *Brain*, 117(1):199, 1994.
- [11] E. Grenier H. Gilquin M. A. Dronne, S. Descombes. Examples of the influence of the geometry on the propagation of progressive waves. *Mathematical and Computer Modelling*, 49(11-12):2138–2144, 2009.
- [12] S. J. Boniface C. L. H. Huang M. F. James, J. M. Smith and R. A. Leslie. Cortical spreading depression and migraine: new insights from imaging? *TRENDS in Neurosciences*, 24(5):266–271, 2001.
- [13] P.M. Milner. Note on a possible correspondence between the scotomas of migraine and spreading depression of Leão. *Electroencephalography and clinical neurophysiology*, 10(4):705, 1958.
- [14] J. Young A. Friedman P. G. Aitken, J. Jing and G. G. Somjen. Spreading depression in human hippocampal tissue in vitro. *Third IBRO Congr. Montreal Abstr.*, page 329, 1991.